

Thallium-201 for Myocardial Imaging: Appearance of the Normal Heart

David J. Cook, Ian Bailey, H. William Strauss, Jacques Rouleau, Henry N. Wagner, Jr., and Bertram Pitt

The Johns Hopkins Medical Institutions, Baltimore, Maryland

Thallium-201 myocardial perfusion images were obtained from 13 healthy adults after tracer administration both at rest and at maximal stress. On the rest-injected scan, tracer was seen in left ventricular myocardium, liver, and spleen. In two subjects with resting tachycardia, the right ventricular myocardium was slightly visualized after tracer injection at rest. When tracer was administered at stress, the left ventricular activity was more nearly homogeneous and the left ventricle was better defined on the scan. The left-ventricle-to-lung-background activity ratio increased from 2.4 at rest to 3.4 at stress. The right ventricular myocardium was seen on the stress-injected scan. Phantom studies, performed to define the optimum position for visualization of lesions, showed that small lesions were best defined when seen either en face or in tangent. Scans should be performed at stress whenever possible and multiple views are essential.

J Nucl Med 17: 583-589, 1976

Thallium-201 is a monovalent cationic radionuclide whose initial cardiac distribution after intravenous administration parallels myocardial perfusion (1). Images recorded after intravenous administration of ^{201}Tl have been used to detect both myocardial infarction (2) and transient myocardial ischemia in man (3). The 69-80-keV x-rays emitted by this tracer permit imaging with high-resolution low-energy collimators, which are not practical with potassium or rubidium (Table 1). These higher-resolution images have revealed patterns of nonhomogeneity

of tracer distribution in normal subjects that were not readily apparent in studies recorded with potassium or rubidium. This finding led us to evaluate a series of subjects without evidence of cardiac disease to determine the normal pattern of thallium distribution in the myocardium. The tracer was in-

Received Dec. 19, 1975; revision accepted Jan. 27, 1976.
For reprints contact: H. William Strauss, 615 N. Wolfe St., Baltimore, MD 21205.

TABLE 1. SEVERAL RADIONUCLIDES SUGGESTED FOR MYOCARDIAL IMAGING: COMPARISON OF HALF-LIVES, GAMMA ENERGY, ABUNDANCE, SUGGESTED COLLIMATION, AND INTRINSIC PHOTOPEAK EFFICIENCY FOR 1.25-cm NaI CRYSTAL

Radionuclide	$t_{1/2}$ (hr)	Gamma energy (keV)	% Emission	Collimation	ϵ^*
^{42}K	22.4	372, 396, (620)	85 (81)	High energy	0.20
^{132}Cs	32	372	32	High energy	0.20
$^{132}\text{N-NH}_3$	0.17	511	180	High energy	0.12
$^{134\text{m}}\text{Cs}$	2.9	128	14	Low energy	1.0
^{201}Tl	72	69-82 (x-ray) 135, 167 (gamma)	90 10	Low energy	1.0

* The approximate photopeak detection efficiency for 11×0.5 -in. NaI crystal [Anger HO (4)].

jected both at rest and during maximum exercise stress to establish criteria for differentiating myocardial perfusion features seen in normal subjects from those seen in heart disease.

MATERIALS AND METHODS

Thallium-201 myocardial perfusion scans were performed on 13 healthy volunteers: 12 men and one woman, average age 35 years, range 21–54, without any previous history or current evidence of cardiovascular disease. All were normotensive, and all chest radiographs were normal, as were the ECGs, both at rest and under maximum stress. Scans were performed on two separate occasions: (A) after injection of tracer at rest, and (B) after injection after graded upright bicycle exercise, using a standard protocol, until at least 90% of maximum predicted heart rate was reached. One patient was exercised twice (the first time to maximum, and the second time to 70% of maximum) to evaluate the scan changes caused by intermediate exercise. All electrocardiograms at stress were recorded using a multi-lead system. For the rest injection, 1 mCi of ^{201}Tl (as thallous chloride, Philips-Duphar or New England Nuclear) was administered intravenously with the subject in the upright position to reduce hepatic blood flow and hepatic concentration of tracer. For the exercise examination, the agent was administered at the time of maximum stress through an indwelling venous catheter kept patent by slow infusion of normal saline. The level of exercise was kept constant for at least 30 sec after tracer administration to prolong the steady state of regional myocardial perfusion while most of the tracer was being cleared from the blood.

Following injection, the subjects were placed supine on a stretcher and imaging commenced 5–10 min later. Myocardial scans were recorded with an Ohio-Nuclear Series-100 scintillation camera using a high-resolution low-energy parallel-hole collimator. Subjects remained supine throughout the procedure and the detector of the scintillation camera was rotated to record the anterior and 45° and 60° left anterior oblique views. A 20% window centered on the mercury x-ray peak (69–80 keV) was used rather than on the less abundant gamma peaks at 135 and 167 keV. (An instrument with dual pulse-height analyzers would permit these higher-energy photons to be utilized in addition to the x-ray peak, with improvement in the count rate and perhaps also some improvement in resolution.) Fifty thousand counts were accumulated from the region of the myocardium in 8–12 min per view (about 200,000–300,000 total counts per image). This resulted in a count density of at least 1,000 counts/cm² over the

region of the myocardium. Images were recorded both directly onto 35-mm film from the camera's oscilloscope and into an Ohio-Nuclear Series-150 data system from which, after uniform field correction, the data were stored on magnetic tape.

The scans were evaluated both by visual inspection of the data (as photographed from the data system with 25% contrast enhancement) and by measurement of count densities using 1-cm² regions of interest placed over the myocardium and adjacent lung background. The shadow of a 10-cm lead marker, placed on the patient's chest during image recording, was used as a reference for correction of all myocardial thickness measurements to life size. The thickness of the left ventricular wall was measured from images at the midportion of the anterolateral surface, inferior surface, septum, and posterior wall.

To determine the effect of cardiac motion on the appearance of the myocardial scan, an anesthetized 20-kg dog was administered 3 mCi of ^{201}Tl intravenously. Scans were recorded in the anterior position, ungated, and also ECG-gated to record only (A) during the last 50 msec of the T wave (corresponding to end systole), and (B) during the 50 msec preceding the next R wave (end diastole), as previously described for gated blood pool imaging (5). Fifty thousand counts were recorded over the region of the myocardium for each of the images. The gated images required ten times longer to record than the ungated images.

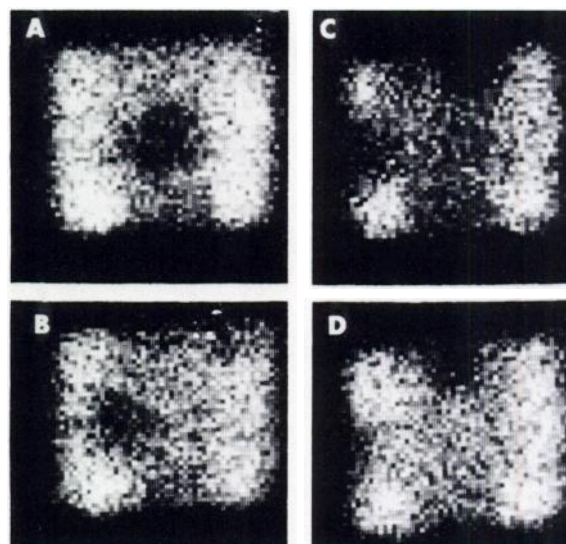


FIG. 1. Phantom scans with 2.5-cm lesion located in midportion of phantom and 1.5-cm lesion located near top. (A) Larger (2.5-cm) lesion is seen en face (0°), while smaller lesion is located toward back of phantom. (B) Larger lesion has rotated 45° to left, which brings smaller lesion faintly into view. (C) Larger lesion has rotated so that it is seen in tangent (90°), while smaller is almost en face. (D) Larger lesion rotated to 105°, while smaller is seen en face.

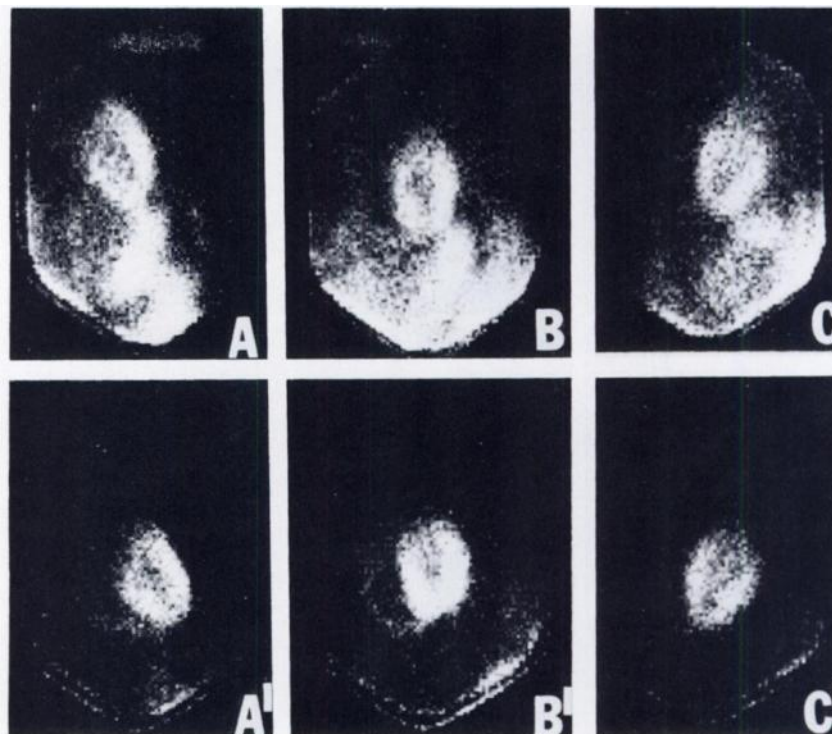


FIG. 2. (Top) Rest-injected scans; (bottom) exercise-injected. (A,A') Anterior position; (B,B') 45° LAO; (C,C') 60° LAO. Region of decreased activity is shown at apex of left ventricle. Activity below left ventricular myocardium, seen in rest study, is mostly in liver and spleen. When tracer is injected at maximal exercise, splanchnic activity is markedly reduced. Similarly, pulmonary activity is reduced and left ventricular myocardium is better defined. Region of reduced tracer activity at apex is still clearly defined and is probably caused by thinning of ventricle. Region of increased tracer concentration at lower septum and midposterior wall (frames B' and C') corresponds to insertion of papillary muscles.

Phantom studies. To determine the limits of resolution and the optimal positions for detecting lesions, images were made with a myocardial phantom. The phantom was composed of two concentric glass beakers, the smaller (150 ml) being suspended inside the larger (250 ml). The space between the two vessels simulated the myocardium and was filled with 100 μ Ci of ^{201}Tl . The inner beaker, simulating the cardiac chamber, was filled with water, which served as an absorber and simulated tracer-free blood in the cardiac chamber. Two full-thickness wax "lesions" were placed in the space between the two vessels: the larger was 2.5 cm in diameter and the smaller was 1.5 cm. To simulate scatter through the chest wall, 2 cm of Lucite was placed in front of the phantom. To simulate background activity in the lung and chest wall, a sheet source measuring $30 \times 30 \times 1$ cm was filled with 100 μ Ci of ^{201}Tl and placed behind the cardiac phantom. Images of the phantom were recorded for 50,000 counts over the region of the beakers in multiple views, 15° apart, from 0° to 180°. The resultant scans were analyzed visually to determine the positions in which the lesions were best visualized.

The camera system's resolution for thallium was compared to that for technetium by imaging an Anger "pie" phantom with the low-energy high-resolution collimator, using first a technetium and then a thallium sheet source with 20% windows at 140 and 75 keV, respectively.

RESULTS

Phantom studies. The 2.5-cm lesion was seen in all positions but was best visualized either en face or in tangent (Fig. 1). It was not visualized if the lesion was rotated to the back of the phantom. The 1.5-cm lesion was best seen at 0° (en face) and was poorly defined at 90° (in tangent). This lesion was very difficult to see in all other positions. In the Anger pie phantom study, all six quadrants of the phantom were defined at the technetium energy, but only four quarters were well resolved at the thallium energy.

CLINICAL STUDIES

Electrocardiogram. The electrocardiograms were normal in all subjects both at rest and during maximum exercise stress.

Scan following injection at rest. Whether at rest or following stress, ^{201}Tl activity within the heart was seen only in the ventricular muscle. The ratio of left ventricular activity to lung activity increased from 2.5 ± 0.3 (s.d.) to 3.4 ± 0.7 during exercise. Absolute counts from the myocardium (activity in the heart minus background) increased only 10% between rest and stress. The ratio of left ventricular activity to liver activity also increased as a result of exercise, going from 1.2 ± 0.2 to 2.9 ± 0.4 . When tracer was injected during exercise, the ventricular walls were more sharply demarcated than when tracer was administered at rest. With the tracer dose

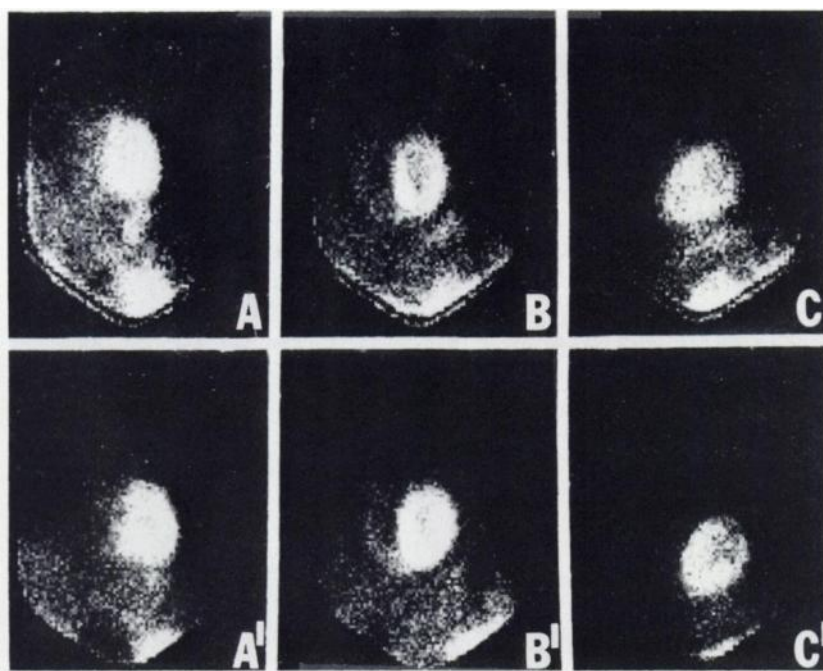


FIG. 3. (Top) Rest-injected scans; (bottom) injected at submaximal stress. (A,A') Anterior position; (B,B') 45° LAO; (C,C') 60° LAO. Right ventricular myocardium is barely visible in rest-injected scan in 45° LAO position (B). Midportions of septum and posterior wall are prominent, probably due to insertion of papillary muscles. In scan injected at submaximal stress, activity is still seen to slight degree in splanchic region, right ventricular wall has become more prominent, and distribution of tracer within myocardium is more homogeneous.

employed, the time taken for each view was approximately 10 min; this required a total time of 40 min to complete the images. There was no significant difference between the rest and stress studies in regard to the imaging time required.

Rest (anterior view). The left ventricular anterolateral wall, apex, and inferior wall were well seen in this view. The left ventricular cavity appeared as a region of reduced activity between these structures (Figs. 2 and 3). The right ventricle and septum were not well seen. The left ventricular anterolateral wall and the inferior wall appeared as two bands of activity extending in arcs between the base of the heart and the apex of the left ventricle. In 7 out of 13 studies, these arcs tapered slightly a short distance from the apex. In these seven subjects the apex appeared as a well-defined zone of reduced activity. The two walls generally appeared to be of comparable thickness, and in 6 cases out of 13 they concentrated activity to a similar degree. The inferior wall was more prominent in 6 out of 13, and the anterolateral wall in only 1 out of 13. Near the base of the heart, the activity in the anterolateral wall (10 out of 13) and the inferior wall (8 out of 13) appeared to taper and became less distinct. The dimensions of the left ventricle as visualized in the anterior projection are given in Table 2.

Rest (45° left anterior oblique view). This view was the best for visualization of the septum and for estimation of the size of the left ventricular cavity. The septum and posterolateral wall of the left ventricle were seen to extend upward to the region of the mitral and aortic valves (Figs. 2 and 3). The

TABLE 2. APPARENT DIMENSIONS OF THE LEFT VENTRICULAR MYOCARDIUM

View	Mean	s.d.	Range
ANTERIOR			
Average thickness, inferior wall	2.5	0.8	1.4–4.1
Average thickness, anterolateral wall	2.0	0.2	1.9–2.3
Depth at base	6.8	1.0	5.6–8.4
Length of ventricle	7.4	0.8	5.6–8.4
40–45° LEFT ANTERIOR OBLIQUE			
Septum thickness at aortic plane (a)	1.7	0.4	1.4–2.3
Septum thickness at base (b)	2.0	0.3	1.4–2.3
Average postero-inferior wall thickness (i)	2.4	0.3	1.9–2.8
Ratio septal thickness (a/b)	0.9	0.1	0.7–1.0
Ratio (b/i)	0.8	0.15	0.6–1.1

length and shape of the septum was variable. Its length was determined by the position of the aortic valve, while its contour varied from slightly trapezoidal, tapering towards the aortic valve plane (9 out of 13), to uniform thickness throughout (4 out of 13). The ratio of septal width at the aortic valve plane to its width in its distal portion varied from 0.6 to 1.0 (Table 2). When the septum was trapezoidal, its activity decreased uniformly into the valve plane without any abrupt cutoff. With a high aortic valve, the septum appeared longer, with a more abrupt reduction in septal activity at the aortic valve plane. In the majority (7 out of 13) the inferior portion of the septum swept around to form the in-

ferior wall of the left ventricle without any significant discontinuity. In the remaining six the transition was visible, with less activity in the inferior wall of the ventricle than in the distal part of the septum. The inferior wall of the left ventricle blended imperceptibly into the posterolateral wall, ending in the region of the mitral valve, where its termination was either abrupt (5 out of 13) or tapering (8 out of 13). The mitral valve itself produced a region of reduced activity in the upper half of the posterior wall of the left ventricle, but its full extent was variable. Irrespective of its extent, the point of insertion of the mitral valve into the posterior wall was at times associated with a localized reduction in thallium activity (2 out of 13). In 5 out of 13 subjects there was a region of increased thickness about midway down the posterolateral wall of the left ventricle; this probably represented the point of insertion of the papillary muscle.

The right ventricular myocardium was not usually seen in the rest study (11 cases). Slight visualization of the right ventricle occurred in two subjects who had tachycardia at the time of injection of tracer. The amount of activity within the right ventricular free wall was always less than the activity within the septum and left ventricular free wall and was only slightly above background. A small lip of activity extending anteriorly from the inferior portion of the septum was the most frequently seen (7 out of 13) portion of the right ventricular free wall.

Rest (60° left anterior oblique view). This was the best view for visualization of the posterolateral wall of the left ventricle, and it aided in interpreting the other views with respect to the anteroseptal and inferior walls. The anteroseptal, inferior, and posterolateral walls formed a continuous band of activity, with some slight thinning in the anterior part of the inferior wall in five subjects. In 6 out of 13 subjects, there were two regions of increased wall thickness, one in the low anteroseptal wall and the other in the posterior wall. A small lip of right ventricular wall was seen in front of the anteroseptal wall of the left ventricle in most subjects (9 out of 13).

Scan appearance after tracer injection at exercise.

Although the overall pattern of thallium distribution to the left ventricle, and the contour and dimensions of the heart, largely duplicated those of the rest study, certain important differences were found. There was less pulmonary and splanchnic activity and an absolute increase in the myocardial ^{201}Tl uptake in all subjects (see above). The ^{201}Tl distribution throughout the left ventricular myocardium was more homogeneous at stress (13 out of 13). The right ventricular myocardium was visualized in all subjects at stress (Figs. 2 and 3). In the 40° LAO view it was seen to extend anteriorly in an arc from the base of the septum and upwards to the plane of the tricuspid valve. In so doing, it partly enclosed an area at least as large as the area of the left ventricle (area RV/LV = 1.0–1.3).

The effects of cardiac motion on the apparent thickness of the myocardial walls can be appreciated from the dog scan (Fig. 4).

DISCUSSION

The phantom studies with ^{201}Tl suggest that multiple views are essential if small lesions are to be detected. While lesions of 2.5 cm or greater can be seen in any projection, the smaller lesions are often seen best when viewed either "en face" or "in tangent." Because of the relatively low energy of ^{201}Tl , small lesions may be obscured by superimposed overlying or underlying areas of normally perfused myocardium. Conversely, the tracer inhomogeneity seen in normal subjects at the apex of the myocardium might be interpreted as a perfusion defect indicative of ischemic heart disease. An apical zone of decreased ^{201}Tl concentration was seen in 7 of the 13 normal resting subjects. While the decreased apical tracer concentration seen in normal subjects may resemble that seen in patients with documented myocardial infarction and could thus be interpreted as a perfusion defect, there are important differences that allow separation of the normal subjects from those with proven ischemic heart disease. The decrease in activity in acute myocardial infarction is



FIG. 4. In vivo scans of canine heart, including 10-cm lead marker (partially outlined). Apparent thickness of ventricular wall in ungated image (A) is less than that seen in systolic image (B) but greater than that in diastolic image (C). Ventricular cavity appears largest in diastolic image.

relatively abrupt, whereas there is a more gradual decrease in activity near the apex in the normal subjects. The picture in the normal subjects is probably due to anatomic thinning of the heart in this zone. In the normal subjects the appearance of this zone tends to become more uniform during stress, whereas in patients with ischemic heart disease the tracer activity either remains abnormal or decreases further during stress. In addition to decreased tracer concentration at the apex in normal resting subjects, irregularities can be seen in the thickness of the septum and the posterior and inferior walls of the left ventricle. These irregularities are probably due to insertion of the papillary muscles. The anterior papillary muscle protrudes partly from the anterior and partly from the septal wall of the left ventricle, whereas the posterior papillary muscle arises in several parts from the posterior wall (6). The sizes and sites of insertion of these muscles are variable, so that in some individuals they will be seen prominently in the ^{201}Tl scan, whereas in others they will not be seen at all.

One of the problems previously encountered in myocardial perfusion imaging with ^{43}K and ^{81}Rb was intense activity in the liver or stomach, which obscured the inferior border of the heart, making detection of inferior lesions difficult. This problem was not encountered in the present study using ^{201}Tl because of the relatively lower hepatic and gastric uptake of this agent compared with previously used cationic tracers (1).

The measured dimensions of the cardiac image presented in this study are somewhat at variance with the reported thickness (1.5 ± 0.2 cm) of the left ventricle in cadavers (6). There are two principal reasons for this discrepancy: (A) the ^{201}Tl myocardial scan is accumulated during the entire cardiac cycle and thus gives a blurred image of a moving target; and (B) the cardiac wall is not a flat structure viewed on edge but is curved around the central cavity. The excursion of the ventricular wall between diastole and systole tends to set the outer limits of the ventricular walls at the end diastolic position while the inner limits approximate the end systolic position of the endocardium. Cardiac rotation during systole will further tend to increase the apparent dimensions of the muscle wall. The motion artifact introduced in this way may be partially overcome by "gating" the scintillation camera to acquire data only during end systole and/or end diastole. Although gating sharpens the myocardial perfusion image, the total scanning time is increased due to the considerably shortened period in each cardiac cycle during which data are obtained. Patient motion artifacts and acceptability become significant problems in certain circumstances when imaging time is prolonged.

The ovoid shape of the left ventricle tends to decrease the apparent size of the ventricular cavity on the myocardial perfusion scan. The cavity will be seen only when there is sufficient contrast between the walls seen in tangent and the walls seen "en face." The apparent size of the left ventricular cavity, and the apparent wall thickness, will depend on the degree of contrast employed as well as on the anatomy of the ventricle. The measurements obtained from the ungated images should thus be regarded as relative rather than absolute. Nevertheless, such measurements may be of considerable value in helping to differentiate hypertrophic changes and ventricular dilatation from normal conditions (7).

The inability to visualize the right ventricular myocardium on the normal resting perfusion scan probably reflects its smaller mass, thickness, and blood supply. Average right ventricular thickness is about one-third of left ventricular thickness (8). Right ventricular myocardial visualization following injection at stress and during resting tachycardia appears to be related to increased myocardial blood flow under these conditions as well as to a general reduction in background activity.

The usual dose of ^{201}Tl given for cardiac scanning is 2 mCi. Because our volunteers were healthy individuals easily able to tolerate a prolonged scanning period, the dose administered in this study was only 1 mCi per scan. The radiation burden for ^{201}Tl administered intravenously has recently been estimated by Bradley-Moore et al (9). Although the total-body dose is 0.07 rad/mCi, the renal and gonadal doses are greater (kidney, 0.25/mCi; testes, 0.25/mCi) and were major considerations when the smaller standard dose was chosen for our normal volunteers.

Since the ^{201}Tl distribution during stress is more uniform than that at rest and since the scan is easier to interpret because of the lower background activity present at stress, we suggest that the stress scan should be the first study in a patient suspected of ischemic heart disease. If tracer uptake is uniform with injection at maximal stress, a resting scan may not be necessary. If, however, an area of inhomogeneity in tracer distribution is detected at stress, a resting scan is indicated in order to determine whether the perfusion defect noted at stress is present at rest, thus suggesting an area of permanent myocardial damage, or whether it disappears at rest, suggesting an area of transient ischemia.

ACKNOWLEDGMENTS

The authors are grateful to Rolf DeJong of the Philips-Duphar Company for supplying much of the thallium used in this study. We are also grateful to William Schaeffer and

Peter Manspeaker for their technical assistance in the performance of the scans and phantom studies.

This work was supported under USPHS Grant GM-10548 and Grant PH-43-NHLI-167-144 from the National Institutes of Health. Dr. Cook is supported by a Clinical Research Fellowship from the Post-Graduate Committee in Medicine from the University of Sydney.

REFERENCES

1. STRAUSS HW, HARRISON K, LANGAN JK, et al: Thallium-201 for myocardial imaging: Relation of thallium-201 to regional myocardial perfusion. *Circulation* 51: 641-645, 1975
2. WACKERS FJ, SCHOOT JB, SOKOLE EB, et al: Non-invasive visualization of acute myocardial infarction in man with thallium-201. *Br Heart J* 37: 741-744, 1975
3. BAILEY IK, GRIFFITH LSC, STRAUSS HW, et al: Detection of coronary artery disease and myocardial ischemia by electrocardiography and myocardial perfusion scanning with thallium-201. *Am J Cardiol* 37: 118, 1976
4. ANGER HO: Radioisotope cameras. In *Instrumentation in Nuclear Medicine*, Hine GJ, ed. New York, Academic, 1967, p 506
5. STRAUSS HW, ZARET BL, HURLEY PJ, et al: A scintigraphic method for measuring left ventricular ejection fraction in man without cardiac catheterization. *Am J Cardiol* 28: 575-580, 1971
6. LATIMER HB: The weight and thickness of the ventricular walls in the human heart. *Anat Rec* 117: 713-723, 1953
7. BULKLEY BH, ROULEAU J, STRAUSS HW, et al: Idiopathic hypertrophic subaortic stenosis: Detection by thallium-201 myocardial perfusion imaging. *N Engl J Med* 293: 1113-1116, 1975
8. WARWICK R, WILLIAMS PL: 'Angiology. In *Gray's Anatomy*, 35th ed. Philadelphia, W. B. Saunders, 1973, p 602
9. BRADLEY-MOORE PR, LEBOWITZ E, GREENE MW, et al: Thallium-201 for medical use. II. Biological behavior. *J Nucl Med* 16: 156-160, 1975

New MIRD Committee Publications

Pamphlet #1, Revised—A Revised Schema for Calculating the Absorbed Dose from Biologically Distributed Radionuclides—12 pp.

Describes how to calculate the radiation dose and establishes a mathematical formalism for simplifying dose calibrations. This number is a revision of Pamphlet #1, which was first published February 1968 as part of MIRD Supplement #1. It introduces the term "S," the absorbed dose per unit cumulated activity, and offers more information on the requirements of a kinetic model.

\$6.75 with binder; \$4.50 without binder.

Pamphlet #10—Radionuclide Decay Schemes and Nuclear Parameters for Use in Radiation-Dose Estimation—Approx. 125 pp.

Provides essential radioactive decay scheme information in convenient form on more than 120 medically important radionuclides. This publication updates and supersedes Pamphlets 4 and 6 which provided data for 54 radionuclides. In loose-leaf binder format for ease of updating and adding additional radionuclides.

\$8.75 with binder; \$6.50 without binder.

Pamphlet #11—"S" Absorbed Dose per Unit Cumulated Activity for Selected Radionuclides and Organs—Approx. 255 pp.

The tabulated values of "S" in this publication simplify dose calculations. Instead of requiring separate consideration of each radiation of the decay scheme and its associated absorbed fraction, the "S" tabulation permits dose calculations by simply referring to a single table entry for each organ combination. This pamphlet provides "S" values for 117 radionuclides plus 6 parent and short-lived daughter combinations as a uniformly distributed source in 20 source organs irradiating 20 target organs which include ovaries, red bone marrow, testes, and total body. In loose-leaf binder format for ease of updating and adding additional radionuclides and source and target organs.

\$10.20 with binder; \$7.95 without binder.

Extra binders available at \$3.75 each.

Please address all orders to:

MIRD Pamphlets
Society of Nuclear Medicine
475 Park Avenue South
New York, N.Y. 10016

CHECKS MADE PAYABLE TO THE "SOCIETY OF NUCLEAR MEDICINE" OR A PURCHASE ORDER MUST ACCOMPANY ALL ORDERS.